THE BEAM DYNAMICS DESIGN FOR J-PARC LINAC ENERGY UPGRADE

M. Ikegami *, H. Ao, Y. Yamazaki, KEK, Tsukuba, Japan
T. Morishita, H. Sako, JAEA, Tokai, Japan

Abstract

We will have an energy upgrade for J-PARC linac, where ACS section is added to increase the output energy from 181 MeV to 400 MeV. The beam dynamics design of ACS and the matching section to it is revised to reflect the recent results of R&D studies. The revised design is presented with some preliminary simulation results.

INTRODUCTION

J-PARC (Japan Proton Accelerator Research Complex) is a high-intensity proton accelerator facility which consists of an injector linac, 3-GeV RCS (Rapid Cycling Synchrotron), and 50-GeV MR (Main Ring) [1]. While the output beam energy of J-PARC linac is currently 181 MeV, we have planned an upgrade of the linac output energy to 400 MeV to ease the space-charge effects in the RCS injection process [2]. The upgrade will be realized by adding ACS (Annular Coupled Structure linac) section after existing SDTL (Separate-type Drift Tube Linac) section [2, 3]. The ACS part was originally in the scope of the first phase of the project, but its construction has been postponed due to a budgetary situation. An additional budget for the construction of the ACS part has recently been approved by the government, and its construction has been started since this March.

As the recent results in the ACS R&D study has already been reported [3], we focus in this paper on the beam dynamics design on the ACS section and the matching section between SDTL and ACS. In the matching section, to which we refer as MEBT2 (Medium Energy Beam Transport 2), we have two buncher cavities for the longitudinal matching. We also have a debuncher system in the transport line after ACS, but its beam dynamics design is discussed in a separate paper [4]. The assumed tuning scenario for ACS and related beam monitor layout are also discussed in another paper [5].

The original design for ACS was presented in LINAC'02 [6]. The present design of ACS is mostly based on the 2002 design, but we have performed some modifications for further optimization guided by the advances in the recent R&D efforts. In this paper, we summarize these modifications and present some particle simulation results for the revised design.

* masanori.ikegami@kek.jp

DESIGN MODIFICATIONS FOR ACS

The ACS is a variety of CCL's (Coupled-Cavity Linacs), which is operated with the $\pi/2$ mode. The distinctive features of ACS are discussed in the reference [7]. An ACS module consists of two ACS tanks connected with a bridge coupler as shown in Fig. 1. The RF power is fed through an input coupler located in the middle of the bridge coupler. Quadrupole doublets are placed at the inter-tank spacing for the transverse focusing. The operation frequency for ACS is chosen to be 972 MHz, which is three times as high as that for the upstream SDTL. The RF power is fed by a 3-MW klystron developed for ACS [8]. The main specifications for ACS is summarized in Table 1, where the values in parentheses are those after further upgrades [2]. We plan to start the ACS operation with the peak current of 30 mA and the repetition rate of 25 Hz.

Comparing Table 1 with the corresponding one in the reference [6], you can find some modifications in main parameters. At first, the number of accelerating cells in a tank is increased from 15 to 17 to reduce the cost for RF sources. Consequently, the number of modules, and hence the number of klystrons also, are reduced from 23 to 21. This modification sacrifices the margin for the RF power by 5 %, but we still have a reasonable margin for stable klystron operation. The increase in the number of accelerating cells also results in a longer focusing period. The focusing period is increased from $12\beta\lambda$ to $13\beta\lambda$ with β and λ being the beam velocity scaled by the speed of light and the RF wave length of 972 MHz, respectively. This change in the period length slightly affects the design of the matching section as discussed later.

Secondly, the average accelerating field is slightly decreased from 4.26 MV/m to 4.12 MV/m to ease the load for the RF sources. In spite of the reduction in the average accelerating field, the maximum surface field is increased

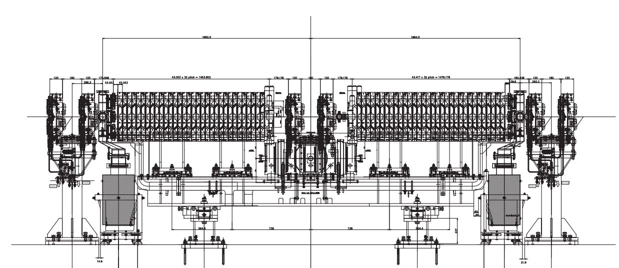

Figure 1: Layout of an ACS module.

from 0.85 Kilpatric to 1.0 Kilpatric. This increase results from a geometry modification for efficient machining. The detailed design of the ACS cavity has been under design polishing for mass production. The main motivation for the design optimization is cost reduction. In particular, reducing the labor for the frequency adjustment is a key to cost saving. In this context, the beta grouping for the ACS tanks have been modified to save fabrication cost. In the revised configuration, two ACS tanks in an ACS module has the same geometrical beta instead of having a different geometrical beta for each tank. This modification results in an increase in the phase slip. In the original design where the geometrical beta is different for each tank, the phase slip is from ± 1.5 deg (the first tank) to ± 0.75 deg (the last tank). Meanwhile, it will be from ± 6.2 deg (the first module) to ± 3.0 deg (the last module) with two-tank grouping. As the longitudinal zero-current phase advance is relatively small (from 37 deg to 25 deg) and the beam is supposed to be safely in the linear regime even with the increased phase slip, we have decided to tolerate the extended beta grouping.

Three of 21 modules (module #1, #10, and #21) have already been fabricated in the course of R&D study, where one-tank grouping is adopted. As they are successfully fabricated, we plan to utilize these modules for actual operation. Then, the two-tank grouping will be adopted in the remaining 18 modules.

The specifications for the quadrupole magnets are determined to enable an equipartitioning setting. The required quadrupole strength for the equipartitioning setting is dependent on the assumed emittance, and it is higher for larger longitudinal-to-transverse emittance ratio. To have a sufficient margin, the required quadrupole strength is determined so that the equipartitioning setting can be realized with more than 50 % emittance growth in the longitudinal direction from an ideal case. The corresponding transverse zero-current phase advance is around 80 deg at the first module and 55 deg at the last one.

Table 1: Main Specifications for ACS

Input beam energy	190.8 MeV
Output beam energy	400 MeV
Operation frequency	972 MHz
Ion species	Negative hydrogen ion
Peak beam current	30 mA (50 mA)
Pulse width	0.5 msec
Repetition	25 Hz (50 Hz)
Num. of cells per tank	17
Num. of tanks per module	2
Num. of modules	21
Num. of klystrons	21
Inter-tank spacing	$4.5\beta\lambda$
Bore radius	20 mm
Average accelerating field E_0	4.12 MV/m
Synchronous phase	30 deg
Max. surface field	1.0 Kilpatrick
Peak rf power	38.3 MW (42.5 MW)
Peak wall loss	32.0 MW
Peak beam loading	6.3 MW (10.5 MW)
Total length	107.1 m

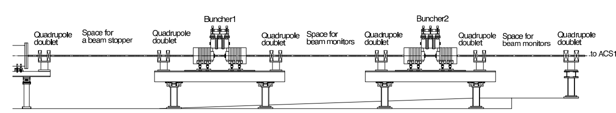

Figure 2: Schematic layout of MEBT2.

DESIGN MODIFICATION FOR MEBT2

Following the design modification of ACS, the design of MEBT2 has also been slightly modified. The main role of MEBT2 is to smoothly absorb the effect of three-fold frequency jump between SDTL and ACS. The period length is also suddenly changed from $21\beta\lambda$ to $13\beta\lambda$ at this transition. In the 2002 design, we adopt "a quasi-periodic lattice" to absorb the transient effects, where the period length is gradually reduced. We basically follow this scheme in the present design, but its actual geometry is slightly modified to cope with the change in the ACS period length.

Figure 2 shows the schematic layout of MEBT2, which consists of six doublet quadrupoles and two buncher cavities. The quadrupole doublets form five "periods" of quasi-doublet lattice, where the period length is linearly reduced from $21\beta\lambda$ to $13\beta\lambda$. While we plan to start the beam operation with reduced number of power sources, a numerical study shows that independent powering of quadrupole doublets is effective in improving the smoothness of the envelope along MEBT2. To facilitate the future upgrade, we plan to prepare cabling for independent powering for each quadrupole from the beginning.

The design for the longitudinal matching is the same as the 2002 design. A possible solution to cope with the longitudinal matching is to introduce a field ramping to smoothly connect SDTL and ACS [10]. However, it is difficult to have a sufficient smoothness for a three-fold frequency jump with a reasonable sacrifice in acceleration efficiency. Then, we decided to introduce two buncher cavities in MEBT2 without adopting a field ramping for ACS. The buncher cavities have already been fabricated as a prototype for the normal ACS module [3], and we plan to utilize them for actual operation.

PARTICLE SIMULATION

Particle simulations are performed to confirm the soundness of the beam dynamics design. We used to mainly use PARMILA [11] for the particle simulation, and an extensive study was performed for the ACS with PARMILA. However, we are now shifting from PARMILA to IMPACT [12] to realize more elaborated and detailed modeling in an effort to analyze the operational data in more accurate ways. For example, we have introduced a real-

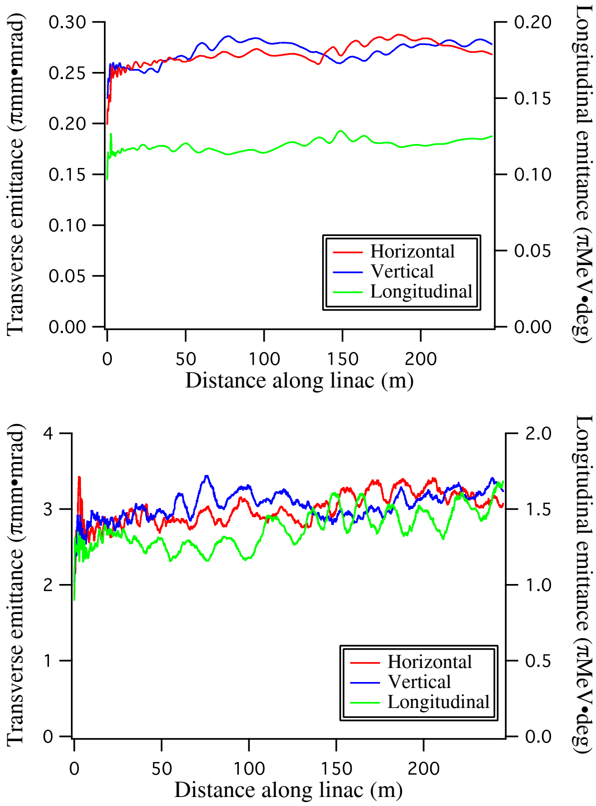

Figure 3: Evolution of rms (top) and 99 % (bottom) emittance along the linac.

istic fringe field for quadrupole magnets in the IMPACT modeling, which we believe essential for accurate modeling especially in the low energy region. Therefore, we here show some IMPACT results instead of obsolete ones with PARMILA, while they are still preliminary.

Figures 3 and 4 show the result of IMPACT simulation, where the beam is tracked from RFQ exit to ACS exit. The initial Gaussian distribution is assumed in this simulation. A 3D mesh with 32x32x64 grids is employed with modest 12,800 macro-particles. The peak current of 30 mA is assumed, and no error is introduced.

While some longitudinal tail arises at the SDTL-ACS transition, the transitional effect is confirmed to be rather modest. As the basic soundness of the design has been confirmed in the simulation, we are planning to proceed to a systematic error study with an increased number of macro-particles and more realistic initial distribution.

SUMMARY

The beam dynamics design of ACS has been modified from the 2002 design, reflecting the advances in the R&D study and the requirement for the cost reduction. The design of MEBT2 has also been modified slightly to cope with the change in the ACS period length. The soundness of the design has been confirmed with preliminary IMPACT simulations, which will be followed by a systematic error analysis in a larger scale.

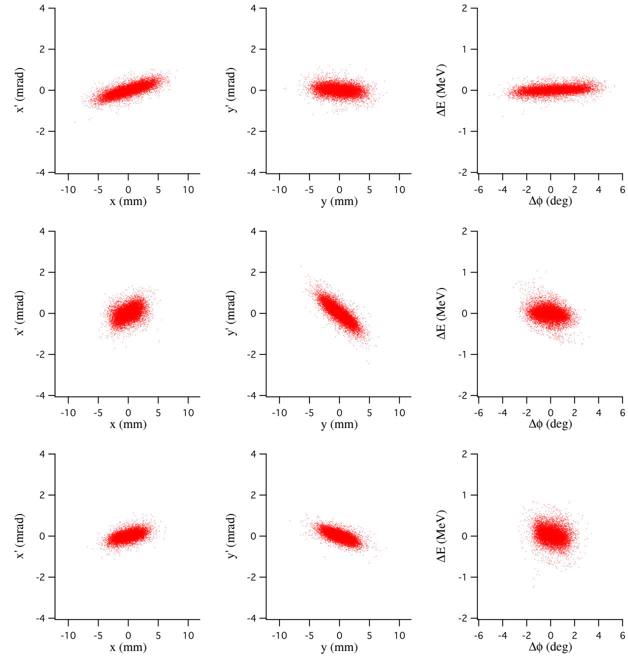

Figure 4: Simulated particle distribution at 181 MeV (top), the ACS entrance (middle), and the ACS exit (bottom).

REFERENCES

[1] Y. Yamazaki, “Status of J-PARC”, in these proceedings.

[2] M. Ikegami, “Progress in the Beam Commissioning of J-PARC Linac and Its Upgrade Path”, LINAC’08, Victoria, September 2008, MO201 (2008).

[3] H. Ao, et. al., “Improvement in the ACS Cavity Design for the J-PARC Linac Energy Upgrade”, LINAC’08, Victoria, September 2008, THP056 (2008).

[4] M. Ikegami, et. al., “Beam Dynamics Design of Debuncher System for J-PARC Linac Energy Upgrade”, in these proceedings.

[5] H. Sako, et. al, “Design of Beam Monitor Configuration for Upgraded 400-MeV J-PARC Linac”, in these proceedings.

[6] M. Ikegami, T. Kato, K. Hasegawa, “Beam Dynamics Design of the Annular-Coupled-Structure Linac and Its Matching Section for the KEK/JAERI Joint Project”, LINAC’02, Gyeongju, August 2002, p. 631 (2002).

[7] T. Kageyama, et. al., “Development of Annular Coupled Structure”, LINAC’94, Tsukuba, 1994, p. 248 (1994).

[8] E. Chishiro, et. al., “Recent Status of RF Source in J-PARC Linac”, PAC’05, Knoxville, May 2005, p. 1123 (2005).

[9] V. V. Paramonov, private communication.

[10] R. Duperrier, et. al., Phys. Rev. ST Accel. Beams 10, 084201 (2007).

[11] H. Takeda, “PARMILA”, Los Alamos National Laboratory Report, LA-UR-98-4487 (1998).

[12] J. Qiang, et. al., J. Compt. Phys. 163, p. 434 (2000).